SPE 114222-PP

A Method for Characterization of Flow Units Between Injection-Production Wells Using Performance Data

Kun-Han Lee (SPE), Antonio Ortega, Amir Mohammad Nejad (SPE), and Iraj Ershaghi, SPE, University of Southern California

Abstract

This paper presents a novel data mining method to characterize the flow units between injection and production wells in a waterflood, using carefully implemented variations in injection rates. The method allows the computation of weight factors representing the influence of any of the injectors surrounding a given producer. The weight factors are used to characterize the effective contribution of injection wells to the total gross production in surrounding production wells. A wavelet approach is used to design the perturbation in the injection rates and to analyze the observed variations in the gross production rates.

Tracking the contribution of injectors to various producers can help in balancing voidage-replacement in waterflood optimization. A second application is reservoir characterization, where information provided by the proposed procedure can help in mapping high permeability flow units such as channels and fractures as well as flow barriers between wells. The method was successfully calibrated and tested for simulated line drive and five spot patterns with various assumed flow units and flow heterogeneity conditions. The paper also includes a case study for a tight formation waterflood where the weight factors are intended to delineate the pattern of natural fractures causing preferential flows.

Introduction

Injection and production rates are the most abundant data available in any waterflood operation and they often correlate to each other in some complex manner. A variety of methods have been used to compare the rate performance of a production well with the surrounding injectors. In these works, the reservoir is viewed as a system that converts an input signal (injection rate) into an output signal (production rate) and the goal is to analyze input and output signals to extract some important information about the reservoir. Such information is beneficial for waterflood optimization and reservoir characterization.

Heffer *et al.*[1] used Spearman rank correlations to relate injector-producer pairs and associated these relations with geomechanics. Panda and Chopra[2] used artificial neural networks to determine the interactions between injection and production rates. Albertoni and Lake[3] estimated the effective flow units (called interwell connectivity in their work) based on linear model using multiple linear regression (MLR) method. A.A. Yousef *et al.*[4,5] improved this work by building a more complex model, named capacitance model in their work, to describe the relationship between injection and production rates. They also used a parameter to describe the effects of compressibility, in addition to transmissibility, between the injection-production interwell channels. Thiele and Batycky[6,7] estimated the effective flow units using streamline-based workflow. Their approach requires building a complete stream flow reservoir model for the region of interest, which is almost impossible for many real fields.

The key novelty of our work is to propose actively controlling the injection rates, choosing different schedules of injection rates at each injection well, so as to improve the accuracy in the estimation of effective flow units. To the best of our knowledge, we are the first to investigate such an active estimation technique. Note that with current oilfield technology, injection rates are very easy to control remotely, so that applying different injection rate patterns to injection wells can be easily put to practice. The selected injecrtion rate schedules are based on wavelets, a very powerful tool in digital signal processing[8-10]. In our design, the injection rates have zero cross-correlation to each other, so that after observing the production rates at each producer, we can more easily separate the influence of the flow units corresponding to each surrounding injector. Finally a weight is calculated

to represent the effective flow units between each surrounding injector-producer pair.

The new procedure has some advantages over the previous injector-producer influence estimation procedures. By selecting the injection rates to have zero cross-correlation with each other, we can improve significantly the quality of estimation. In techniques where the injection rates are not modified for weight estimation, the injection rate patterns can be highly collinear, so it is very difficult to separate the influence of these injectors based only on production data. Another advantage is that, unlike other procedures, the result always leads to non-negative estimated parameters. Negative parameters cannot be avoided when using other techniques and they often complicate the interpretation of the results (and techniques to eliminate negative values after estimation tend to reduce estimation accuracy).

Our proposed technique has been calibrated with a commercial reservoir simulator (CMG).

Injector-Producer Relationships

In a waterflood, production rates are influenced by changes in bottom-hole flowing pressures and the pressure changes caused by fluid injections. For this work, we focus on the the changes caused by variations in carefully designed water injection rates. To quantify the degree of communication between injectors and producers, we estimate weight factors representing the effective flow units, which in turn denote the influence of surrounding injection fluid.

Injector-Producer Model

There have been various studies to quantify the system model for describing the relationships between injection-production rates. In this paper, we consider a general linear finite impulse response (FIR) model: production rates are partly determined by the linear combination of surrounding FIR filtered version of injection rates. That is, for the production rate $P_j(t)$ of a particular producer j:

$$P_j(t) = \sum_{i=1}^{N_I} \delta_{ij} I'_{ij}(t) \quad + \quad \text{other terms} \tag{1}$$

Where $I'_{ij}(t)$ the FIR is filtered version of injection rate for injection i:

$$I'_{ij}(t) = I_i(t) * h_{ij}(t) = \int_{\tau=0}^{t} I_i(t\text{-}\tau) h_{ij}(\tau) d\tau \tag{2}$$

$h_{ij}(t)$ is the impulse response of the channel between injector i and producer j.

δ_{ij} in equation (1) is the relative weight of producer j for injector i, i.e., the effective flow units between producer j and injector i which seek to estimate.

It is easy to show that although this is a linear model, it can be used to approximate many nonlinear models

developed by other researchers. For example, in streamline simulation, the relationships between injectors and producers described by imaginary streamlines can also be captured by this linear model. The nonlinear capacitance model developed by Yousef et al.[4] can also be represented as a linear model in the discrete form, with the FIR shape having some constraints.

The model in discrete form is:

$$P_j(n) = \sum_{i=1}^{N_I} \delta_{ij} I'_{ij}(n) \quad + \quad \text{other terms} \tag{3}$$

$$I'_{ij}(n) = I_i(n) * h_{ij}(n) = \sum_{m=0}^{L} I_i(n\text{-}m) h_{ij}(m) \tag{4}$$

We will use the discrete form of model for the analysis of our procedure later.

Design of Distinguishable Signals

Suppose now that we can control the inputs (injection rates) to the system, within certain constraints and limitations applicable to the injection wells. If we see the reservoir of interest as a system, the inputs are the injection rates of injectors in our case. Based on the model described in previous section, our goal is to design a set of signals, with the goal that each signal be easily distinguishable from others. This is a typical problems in systems engineering, that is, to find a set of signals that have the following property: each signal in the set is easy to distinguish from (a possibly time-shifted version of) every other signal in the set. First of all, we investigate the "distinguishability" between signals.

One of the most common and useful measures of distinguishability is the mean-squared difference. Two signals are easy to distinguish if and only if the mean-squared difference between them is large. Thus the measure of distinguishability is the quantity: (For simplicity, we consider only those sets of signals that are periodic with period T.)

$$\int_0^T |x(t)-y(t)|^2 \, dt = \int_0^T \left[x(t)^2 + y(t)^2 \right] dt - 2\int_0^T x(t)y(t) dt \tag{5}$$

The first integral on the right-hand side is the sum of the energies of x(t) and y(t), in the range of $0 \le t \le T$. So for fixed signal energy, y(t) is easy to distinguish from x(t) if and only if the quantity:

$$C_{x,y} = \int_0^T x(t)y(t) dt \tag{6}$$

$C_{x,y}$ is small. When $C_{x,y}$ is equal to zero, we often say that x(t) and y(t) are orthogonal. For many applications, such as ours, x(t) and y(t) are received from different paths(channels), so there may be some time delay between them. So the measure becomes:

$$C_{x,y}(\tau) = \int_0^T x(t)\,y(t+\tau)\,dt \qquad (7)$$

Which is obviously the magnitude of the cross-correlation function of x(t) and y(t). Thus our goal becomes to find a set of sequences that exhibit low cross-correlation with all possible time delays.

Haar Wavelet Bases

Wavelet analysis is a powerful mathematical tool that has been applied to many digital signal processing problems.[8] The orthogonal wavelet decomposition aims to represent any signal as linear combination of sets of orthogonal signals, which are called wavelet bases.[9] Under the property of orthogonality, any two signals inside this set have cross-correlation equal to zero if there is no time delay $\tau = 0$. In our work, we are motivated by the orthogonality of orthogonal wavelet bases, and find a subset from the original set of wavelet bases such that the crosscorrelation within this sub-set is also zero or nearly zero *even in the presence of arbitrary time delays between the basis functions*. For simplicity of implementation in a real oilfield, we only consider the simplest orthogonal wavelet bases, i.e., the Haar wavelets, which have the property that the basis functions are piecewise constant (so that essentially the injection rates would have to be adjusted to a series of constant values). Here we only consider the discrete case.

The discrete-time Haar wavelet decomposition[9,10] decomposes a discrete-time signal into a linear combination of two elementary basis functions $h_0(n)$ and $h_1(n)$ (here we ignore the scaling constant because it does not affect our procedure):

$$h_0(n) = \begin{cases} 1 & \text{if } n=0,-1 \\ 0 & otherwise \end{cases} \qquad (8)$$

$$h_0(n) = \begin{cases} 1 & \text{if } n=0 \\ -1 & \text{if } n=-1 \\ 0 & othewise \end{cases} \qquad (9)$$

$h_0(n)$ and $h_1(n)$ are shown in Figure 1. If we extend the bases $h_0(n)$ and $h_1(n)$, we can easily get 2^L orthogonal Haar wavelet bases, for a given positive integer L. Figure 2 shows a $2^3 = 8$ orthogonal basis functions example.

In order to investigate the distinguishability of these Haar wavelet bases candidates, we first re-state the metric for distinguishability using in this paper, that is, discrete cross-correlation of two periodic sequences x(n) and y(n):

$$C_{x,y}(\tau) = \sum_{n=0}^{N-1} x(n)\,y(n+\tau) \quad \tau = 0,1,...,n-1 \qquad (10)$$

where N is the period of x(n) and y(n) if they have the same period. If they have different periods, N is the least common multiple of these two periods.

Using this metric, for an L level Haar wavelet bases, we find that when choosing some specific sequences from the basis set, we can obtain a subset for which the cross-correlation among functions in the subset is zero for any any time shift. These selected sequences are defined as follows (the sequence is periodic with period $N=2^L$):

$$w_1(n) = \begin{cases} 1 & \text{if } n=2k \\ -1 & \text{if } n=2k+1 \end{cases} \qquad k \in Z$$

$$w_2(n) = \begin{cases} 1 & \text{if } n=4k,4k+1 \\ -1 & \text{if } n=4k+2,2k+3 \end{cases}$$

$$\vdots$$

$$w_L(n) = \begin{cases} 1 & \text{if } n=0,1,...,2^{L-1}-1 \\ -1 & \text{if } n=2^{L-1},...,N-1 \end{cases} \qquad (11)$$

for n = 0,1,...,N-1. Figure 3 is an example for the sequence set with period N=16. Here we write this zero cross-correlation property in mathematical form:

$$\forall x(n),y(n) \in \{w_1(n),...,w_L(n)\}$$
$$C_{x,y}(\tau) = 0 \quad \text{for } \tau = 0,1,...,n\text{-}1 \text{ and } x \neq y \qquad (12)$$

As the equations have shown, the selected Haar wavelet bases $\{w_1(n),...,w_L(n)\}$ form a set containing sequences that are highly distinguishable from each other, and we will use the selected set of sequences to construct the desired sequences of injection rates in the next section. Note that for a period $N=2^L$, we can get L sequences, which means that we can separate the influence of L injection rates simultaneously using the selected L sequences.

Non-collinearity property

In oilfields with waterflooding, injection and production rates are the most readily available data. Many procedures that infer oilfield characteristics by analyzing injection and production rates can often be inaccurate because the injection rates in daily operations in real fields usually have strong linear dependencies to each other. This is referred to as the collinearity problem. The effects of collinearity on linear estimation procedures are a well-known problem in statistics[11-13]. Some tools have been developed to measure how collinear the data is, these tools include correlation matrix, condition number[14], variance inflation factor (VIF)[15],…,etc. Under all of these metrics, it can be easily shown that the selected Haar wavelet bases $\{w_1(n),...,w_L(n)\}$ achieve the maximum non-collinearity and therefore the designed injection rates based on selected Haar wavelet bases have much better

non-collinearity than the normal injection rates in daily operations.

Procedure

In our work, we assume that we can control the injection rates of all injectors; all that is required is to switch injection rates from time to time to one of a series of discrete distinct levels. We design a set of injection rates according to the set of selected Haar wavelet bases. Each injection rate has a constant average rate obtained as the sum of a specific Haar Wavelet Basis and a constant injection rate term. That is, for injector i, injection rates $I_i(t)$ will be:

$$I_i(t) = I_{0i} + Aw_i(t) \quad \text{with } A < I_{0i} \quad (17)$$

where I_{0i} is the average value of injection rate for injector i, A is a term that determines the (smaller) amplitude of variations corresponding to the Haar wavelet basis. Figure 4 is an example for a four-injector scenario with designed injection rates with period N=16, $I_{0i} = 100$ bbl/day, A = 20 bbl/day.

From the zero cross-correlation property, if we correlate each production rate with a specific Haar wavelet basis, the variations from other Haar wavelet basis will be totally cancelled out, leaving only the influence of the injector with the specific Haar wavelet basis. To illustrate this we use an example: consider just one producer j, with production rate $P_j(n)$. We calculate the cross-correlation between $P_j(n)$ and a specific Haar wavelet basis w_k, which is assiganed to injector k:

$$C_{P_j w_k}(\tau) = \sum_{n=0}^{N-1} w_k(n) P_j(n+\tau) \quad (18)$$

$$= \sum_{n=0}^{N-1} w_k(n) \sum_{i=1}^{N_I} \delta_{ij} \sum_{m=0}^{L} I_i(n+r-m) h_{ij}(m) \quad (19)$$

$$= \sum_{i=1}^{N_I} \delta_{ij} \left[\sum_{m=0}^{L} \sum_{n=0}^{N-1} w_k(n) I_i(n+r-m) h_{ij}(m) \right] (20)$$

Now, using the zero correlation property of Haar wavlet bases, the cross-correlation of w_k and $I_i(n)$ can be simplifed as:

$$\sum_{n=0}^{N-1} w_k(n) I_i(n+r-m)$$

$$= \sum_{n=0}^{N-1} w_k(n)[I_{0i} + Aw_i(n+\tau-m)] \quad (21)$$

$$= I_{0i} \sum_{n=0}^{N-1} w_k(n) + A \sum_{n=0}^{N-1} w_k(n) w_i(n+\tau-m) \quad (22)$$

$$= \begin{cases} AC_{w_k}(\tau-m) & \text{if } i = k \\ 0 & \text{if } i \neq k \end{cases} \quad (23)$$

This means that the influence from injectors other than k will all become zero, only leaving the influence of injector k. So (18) becomes:

$$C_{P_j w_k}(\tau) = \delta_{kj} \sum_{m=0}^{L} C_{w_k}(\tau-m) h_{kj}(m) \quad (24)$$

$$= \delta_{kj} AC_{w_k}(\tau) * h_{kj}(\tau) \quad (25)$$

The parameter δ_{kj}, which represents the flow liquid weight of injector k to producer j, is our target for estimation. The only non-zero term comes from injector k, but we still need to deal with the term $C_{w_k}(\tau) * h_{kj}(\tau)$, which is the FIR filtered version of $C_{w_k}(\tau)$. In order to remove its effects, we sum the absolute value of $C_{P_j w_k}(\tau)$ with all delays:

$$\sum_{\tau=0}^{N-1} \left| C_{P_j w_k}(\tau) \right| = \delta_{ij} A \sum_{\tau=0}^{N-1} \left| C_{w_k}(\tau) * h_{kj}(\tau) \right| \quad (26)$$

If the filter length L << N, we claim that:

$$\sum_{\tau=0}^{N-1} \left| C_{w_k}(\tau) * h_{kj}(\tau) \right| \approx \text{const.} \quad \text{for all } k \quad (27)$$

So

$$\delta_{kj} \propto \sum_{\tau=0}^{N-1} \left| C_{P_j w_k}(\tau) \right| \quad (28)$$

Using equation (28), we can estimate the relative value of δ_{kj} using only production rate data. Thus effective flow units, which are represented by the relative value of δ_{kj}, can be estimated.

We need to discuss a practical issue related to this procedure: how does manifulation of injection rates manipulation in this procedure affect the normal operation in a real oilfield? To what degree does it affect it? In practice this is a complex problem, because when changing the injection rates, the production rates may change in a complex manner according to all the characteristics of the reservoir. Our procedure reduces the effects to the minimum degree by using I_{0i}, the average value of injection rates. We can set the constant value I_{0i} to the average value under normal operation, which on

average we would expect to lead to minimal changes in overall production, while allowing important reservoir information to be obtained thanks to those smaller variations in injection.

Results
The technique was tested on a simple streamline model and a capacitance model with parameters fitting those of a real waterflood in California. Then the procedure was further calibrated against a commercial reservoir simulator. The results of these applications are presented and discussed in this section.

Application to streamline model
We applied our method to two different injector-producer simulation models, the first one is a streamline simulation.[6,7] Suppose all injector-producer well pairs in the reservoir are connected by a batch of imaginary streamlines, according to a simple streamline simulation model. We arbitrarily set the parameters, including volume and time-of-flight (TOF) for each streamline, in the simulation. For our tests we assign injection rates using our design, and then apply the procedure described above to the output production rates. By comparing the results of our estimation with the effective flow units assigned by these simulations, we were able to evaluate our proposed methods. Line drive (scenario shown in Figure 5) and five spot injection patterns (scenario shown in Figure 6) were applied in the simulations.

Streamline simulation for line drive patterns.
In this simulation, we used a 6-injector/3-producer scenario. The minimum time scale in the simulation is set to an hour, but the sampling rate is set to a day in order to capture the fact that in real fields test production data is more likely to be available on a daily basis (rather than on a shorter time scale). The TOF parameters of streamlines are set according to the streamine simulation in real field, changing from several days to several months. We compared the effective flow units in the simulation with the ones estimated by our procedure, the result is shown in Figure 7. The results prove that our procedure can capture the effective flow units with high accuracy in a simple streamline simulation setting.

Streamline simulation for five spot patterns
In this simulation, we apply our method on five spot injection pattern with 5-injectors/4-producers, the remaining simulation settings are the same as in line drive patterns. The result is shown in Figure 8. As in the line drive case, our procedure can estimate the effective flow units with high accuracy in the five spot injection pattern case.

Capacitance Model with field data fitting
According to A.A. Yousef et al.[3], the injector-producer relationship can be approximated by a "capacitance model". In order to verify our procedure, now suppose the input-output relationships follow the capacitance model. Given the injection rates and production rates data in a segment of an actual water flood in California, we first find the parameters in the capacitance model by field data

fitting, which capture some characteristics of this reservoir. Figure 9 shows the region of interest in the field under waterflood. Figure 10 shows the fitting results for production rates. After finding all parameters, we assign our designed injection rates as the inputs, and we can get the production rates of all surrounding producers according to capacitance model. By analyzing the production rates, we can estimate the effective units flow between all surrounding injector-producer pairs and compare them to the parameters in the capacitance model (relative weight λ_{ij} in capacitance model have the same meaning as effective units flow). The results are shown in Figure 11. The results prove that our procedure can estimate accurately almost all of the effective flow units between well pairs in the capacitance model.

Calibration with a commercial numerical simulator
We applied our method on a numerical simulator, CMG, with a line drive injection pattern with 6-injectors/3-producers scenario. In all cases we simulate two component water and oil fluid systems, and have only vertical wells. Oil viscosity was set to 4 CP. The numerical simulation uses day as the time scale; that is, $\Delta n = 1\,\text{day}$.

1-Homogeneous case
The first case is of a single-layered homogeneous reservoir with an isotropic permeability of 100 md, as shown in Figure 12. The reservoir pressure is set to 1000 psi, BHP in the production well are all set to 800 psi. The injection rates are set as in Figure 13. We change the injection rates frequency in the middle of the observation period because we want to see the difference for setting different injection frequencies into different injectors. The original injectors 1 to 6 are set from highest to lowest frequency. In the middle of the observation period, injector 1 exchanges its injection sequence with injector 4, 2 with 5, and 3 with 6. We separately analyzed each of half period, and the results shown in Table 1 and Figure 14 represent the average of the two half periods. The estimated effective flow units are represented by arrows that start from injector and point to producer in each injector-producer pair. The longer the arrow, the larger value of the effective flow units between the two wells.

Because the reservoir is homogeneous, we expected the estimated effective flow units to be almost symmetric across plane of symmetry and to decrease as the distance between well pairs increase. All resulting estimates match well with the chosen reservoir conditions.

2-Anisotropic case
We consider also a single-layered anisotropic reservoir with permeability of 10 md in x direction and 0.01 in y direction. There is a single fracture in the reservoir, as shown in Figure 15. The injection rates are the same as in the homogeneous case, and the results are averaged on the two individual half periods and shown on Table 2 and Figure 16.

Because the y direction has a very low permeability, we expected most of the flows to be in the x direction. Producer 2 has a fracture across it, so it should receive

almost all of the injection fluid. The results show almost all the flow units come to producer 2, as expected.

3-Multiple fractures case

We also considered a single-layered reservoir with an isotropic permeability of 0.1 md and where there are three fractures with different lengths, as shown in Figure 17. The injection rates are set as in the first two cases, and the results are averaged over the two individual half periods and shown on Table 3 and Figure 18.

There are three fractures with different lengths in the reserovoir, and all lay in about 45 degree direction. From the model, we expected injector 1 and 4 will affect producer 1 the most because the fracture across producer 1 has the longest length. Injector 2 and 5 to producer 2 should be the second one. Injector 3 and 6 will have the smallest flow units to producer 3. The simulation results all agree with what we expected.

Conclusion

We developed a technique to characterize the flow units between injection and production wells in a reservoir by using carefully designed injection rates and observing the production rates of surrounding production wells.

The technique has been validated by applications to streamline model and capacitance model with real data fitting. The results have shown that the procedure can successfully capture the effective flow units between surrounding injector-producer pairs.

The technique was also verified by numerical simulations. We evaluated our method on three different cases, and we showed that our estimated effective flow units match the characteristics of the reservoir in each case.

This procedure provides a practical solution to some limitations of existing analysis methods and can lead to improvements in the accuracy of estimation of flow units. The main advantages of this technique are: 1) it avoids the problem of collinearity between injection rates because the injection rates have zero cross-correlation to each other, and 2) the procedure will never get negative parameters, so that estimated weights are more readily interpreted. Furthermore, because other analysis methods are also based on known injection rates, our procedure could be combined with any of these methods and potentially lead to improvements in the quality of the estimation.

Nomenclature

A = amplitude added on Haar wavelet bases (L^3/t)

BHP = bottom-hole pressure (F/L^2)

$C_{P_j w_k}$ = cross-correlation between P_j and w_k

h_{ij} = equivalent impulse response of channel between injector i and producer j

I_i = injection rate (L^3/t)

I'_{ij} = filtered version of injection rate (L^3/t)

L = number of Selected Haar wavelet bases

N = period of selected Haar wavelet bases

N_I = number of injection wells

P_j = liquid production rate (L3/t)

R = correlation matrix

TOF = time-of-flight

U = condition number

VIF = variance inflation factor

w_k = selected Haar wavelet bases

Greek alphabets

λ_{ij} = weights in capacitance model

δ_{ij} = effective flow units

Subscripts and superscripts

i = injector index

j = producer index

k = selected Haar wavelet bases index

Acknowledgements

References

1. Heffer, K.J., Fox, R.J., McGill, C.A., and Koutsabeloulis, N.C., "Novel Techniques Show Links between Reservoir Flow Directionality, Earth Stress, Fault Structure and Geomechanical Changes in Mature Waterfloods," paper SPE 30711 presented at the SPE ATCE, Dallas, October 22-25, 1995.

2. Panda, M.N. and Chopra, A.K., "An Intergrated Approach to Estimate Well Interactions," paper SPE 39563 presented at SPE India Oil and Gas Conference and Exhibition, New Delhi, India, February 17-19, 1998.

3. Albertino, A., and Larry W. Lake, "Inferring Connectivity Only From Well-Rate Fluctuations in Waterfloods," SPE Reservoir Evaluation and Engineering Journal, vol. 6, p 616, 2003.

4. Yousef, A.A., Gentil, P., Jensen, J.L., and Lake, Larry., "A Capacitance Model to Infer Interwell Connectivity from Production and Injection Rate Fluctuations," presented at the SPE Annual Technical Conference and Exhibition held in Dallas Texas, October 9-12, 2005.

5. Yousef, A.A. and Lake, Larry, "Analysis and Interpretation of Interwell Connectivity From Production and Injection Rate Fluctuations Using a Capacitance Model," presented at SPE Symposium on Improved Oil Recovery held in Tulsa, Oklahoma, 22-26 April 2006.

6. Marco R. Thiele, "Streamline Simulation," 6th International Forum on Reservoir Simulation held in Schloss Fuschl, Austria, 3rd-7th September 2001.

7. Marco R. Thiele and Rod. P Batycky, "Water Injection Optimization Using a Streamline-Based Workflow," paper SPE84080 presented at the SPE Annual Technical Conference and Exhibition held in Denver, Colorado, 5-8 October 2003.

8. Daubechies, I. Ten Lectures on Wavelets, Regional Conference Series in Applied Mathematics, Siam, Philadelphia, 1992.

9. Vetterli, M. and Kovacevic, J., Wavelets and Subband Coding, Englewood Cliffs, NJ: Prentice-Hall, 1995.

10. Vetterli, M. and Herley, C., "Wavelet Filter Banks: Theory and Design", IEEE Transactions on Signal Processing, vol. 40 no. 9, New York, September 1992.

11. Snee R., "Development in Linear Regression Methodology," Technometrics, vol. 25, pp. 230-237, 1983.

12. Hocking R., "Development in Linear Regression Methodology," Technometrics, vol. 25, pp. 215-230, 1983.

13. Belsey, D., Conditioning Diagnostics: Collinearity and Weak Data in Regression, Wiley, New York, 1991.

14. Marquardt D. W., "General Inverse, Ridge Regression, Biased Linear Estimation and Nonlinear Estimation," Technometrics, vol. 12, pp. 591-612, 1970.

$$h_0(n)$$

$$h_1(n)$$

$$\sum_n h_0(n)h_1(n) = 0$$
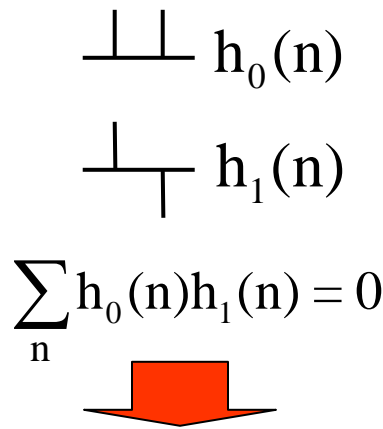
Orthogonal with each other

Figure 1: Haar wavelet bases h0(n) and h1(n) which are orthogonal with each other.

$$h_0(n)$$
$$h_1(n)$$
$$h_2(n)$$
$$h_3(n)$$
$$h_4(n)$$
$$h_5(n)$$
$$h_6(n)$$
$$h_7(n)$$

when $i, j = 0, 1, ..., 7$ and $i \neq j$

$$\sum_n h_i(n)h_j(n) = 0$$

Orthogonal with each other
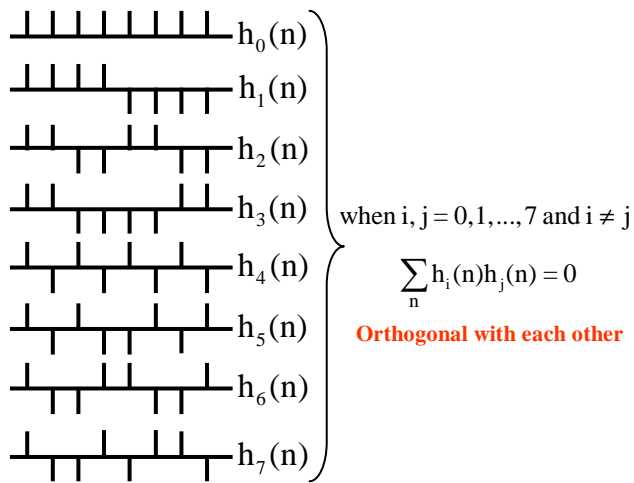
Figure 2: Haar wavelet bases h0(n) ~ h7(n) which are orthogonal with each other.

$$x_1(n)$$
$$x_2(n)$$
$$x_3(n)$$
$$x_4(n)$$
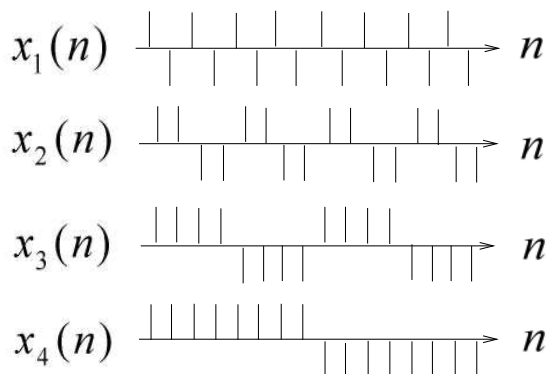
Figure 3: Selected Haar wavelet basis set with period N=16 which perform zero cross-correlation to each other.

Injection Rate for Injector1

Injection Rate for Injector2

Injection Rate for Injector3

Injection Rate for Injector4
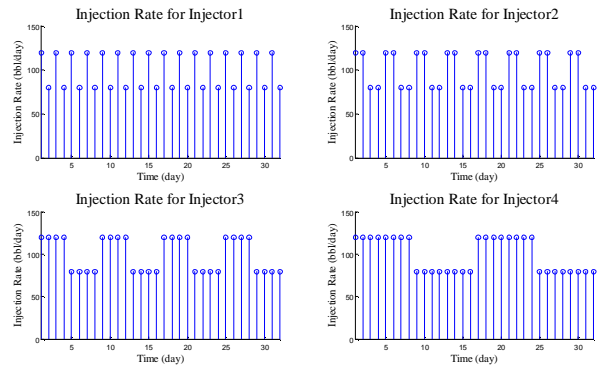
Figure 4: Designed injection rates for four different injectors with period N=16, I_{0i}=100 bbl/day, A=20 bbl/day.

6 injectors/3 producers Line Drive Scenario

▲ Injector 4   ▲ Injector 5   ▲ Injector 6

▲ Injection Well
● Production Well

● Producer 1   ● Producer 2   ● Producer 3

▲ Injector 1   ▲ Injector 2   ▲ Injector 3
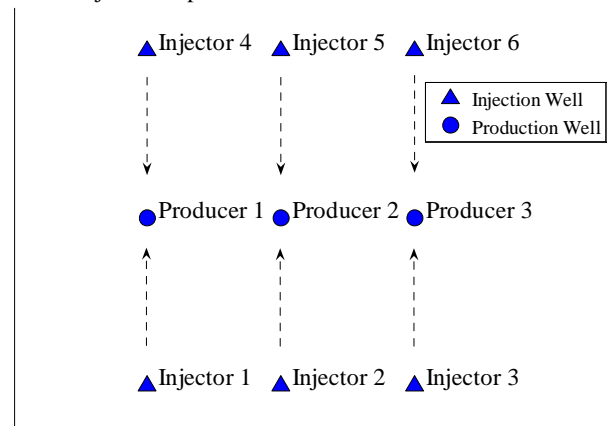
Figure 5: Line drive scenario: 6 injectors and 3 producers.

Five Spot Scenario: 5 injectors/4 producers

▲ Injection Well
● Production Well

Injector 1   Producer 1   Injector 4

Producer 2   Injector 3   Producer 3

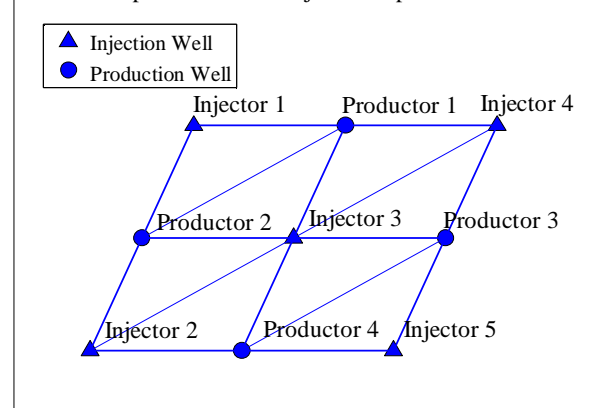Injector 2   Producer 4   Injector 5

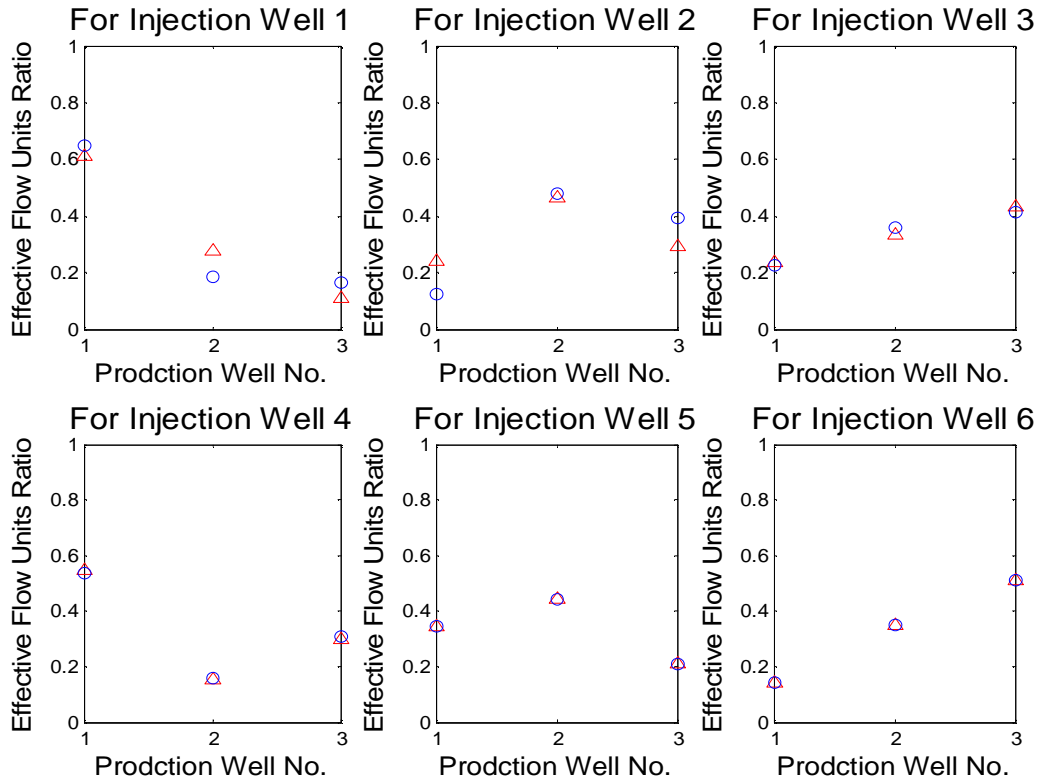**Figure 6: Five spot scenario: 5 injectors and 4 producers.**

Figure 7: The effective flow units in the streamline model (red triangle) and estimated by this procedure (blue circle) in 6 injector/3 producer line drive scenario.
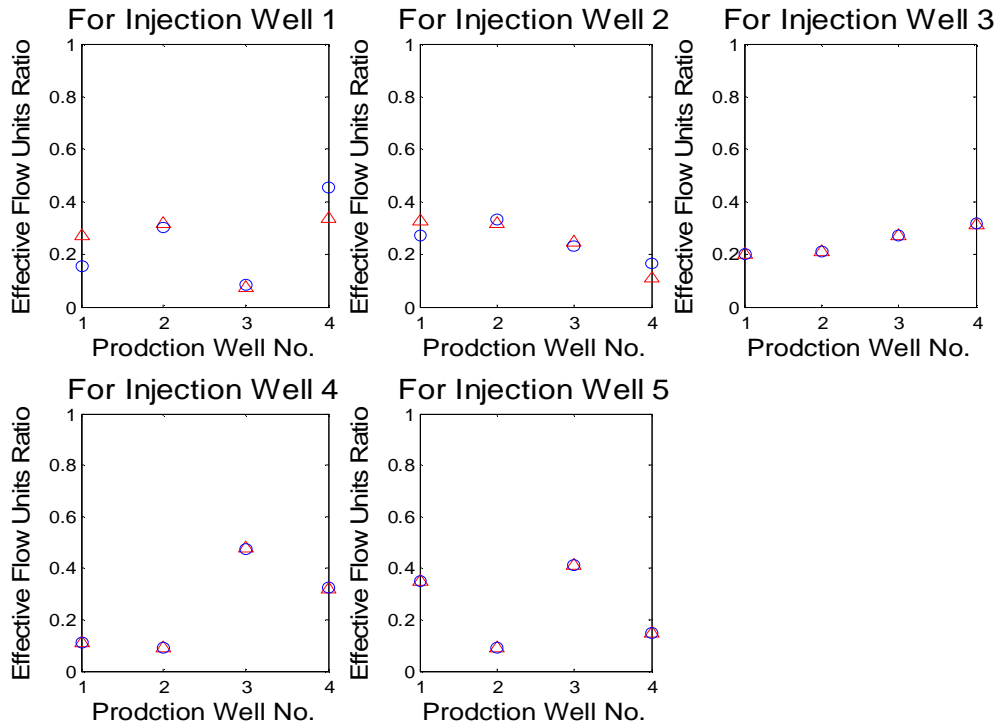

Figure 8: The effective flow units in the streamline model (red triangle) and estimated by this procedure (blue circle) in 5 injector/4 producer five spot scenario.
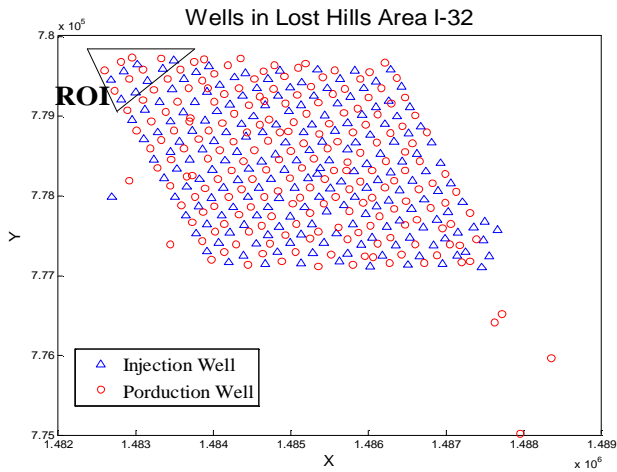
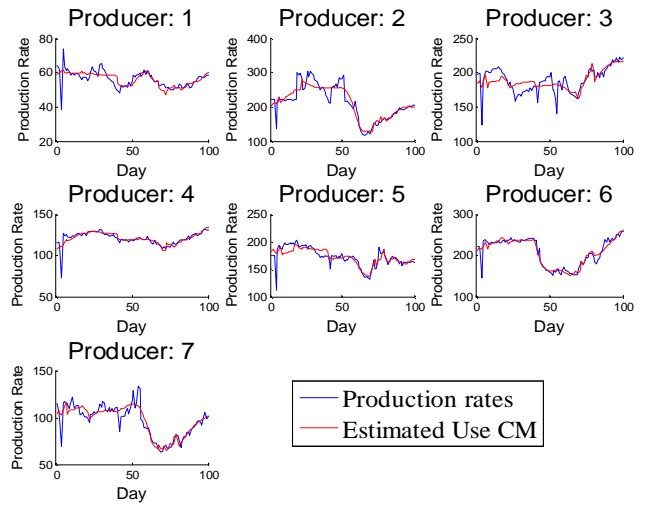**Figure 9: Wells in Field Case Study Area and chosen wells in the region of interest (ROI).**

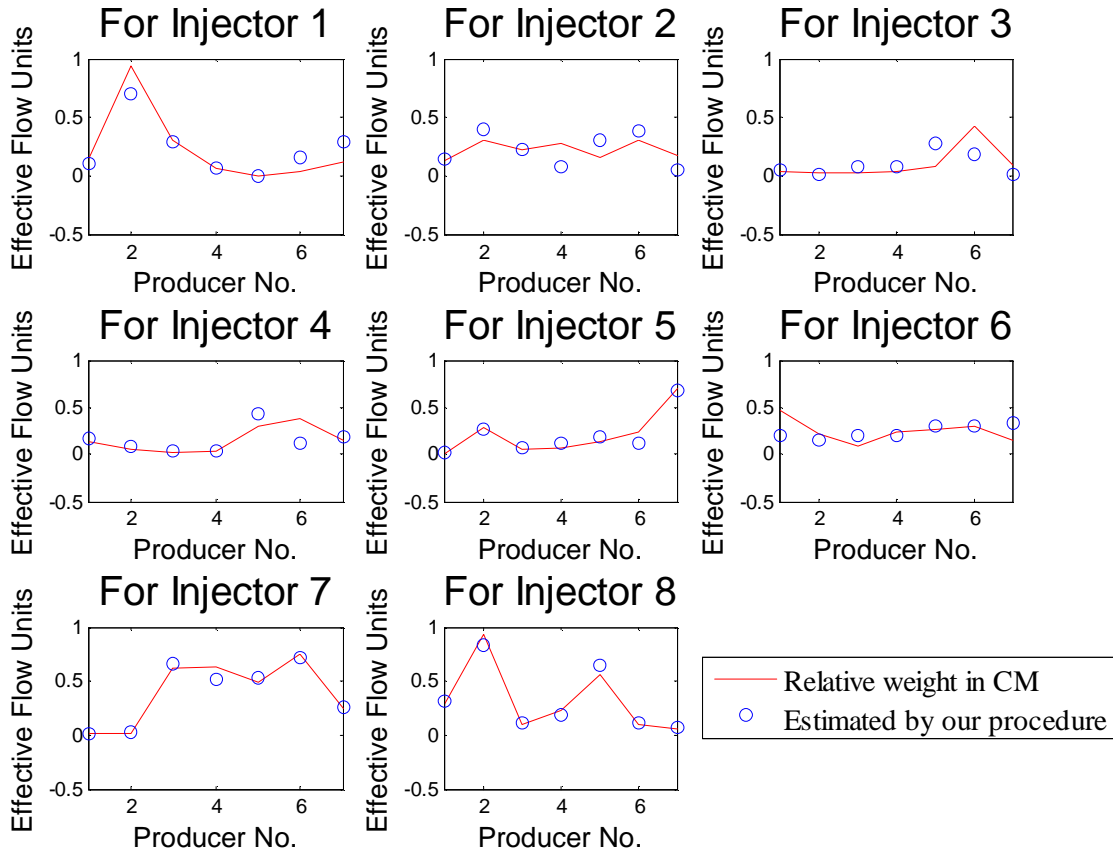**Figure 10: Fitting the production rates in Field Data data using capacitance model.**

Figure 11: The effective flow units in the capacitance model with Field Data data fitting (red line) and estimated by this procedure (blue circle).
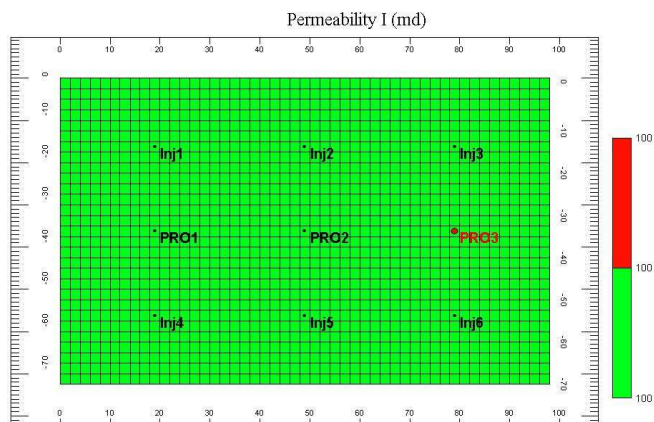
Figure 12: Model on numerical simulator CMG - single layered homogeneous reservoir with an isotropic permeability of 100 md.

Table 1: Estimated effective flow units in homogeneous case plotted in Figure 14.

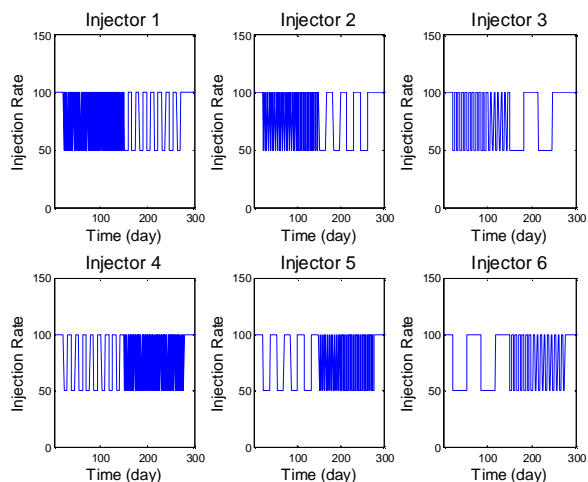|	First half period			Second half period		
	Pro 1	Pro 2	Pro 3	Pro 1	Pro 2	Pro 3
Inj 1	0.523	0.297	0.179	0.507	0.300	0.194
Inj 2	0.304	0.397	0.299	0.313	0.387	0.300
Inj 3	0.191	0.300	0.508	0.214	0.302	0.484
Inj 4	0.507	0.300	0.194	0.523	0.297	0.179
Inj 5	0.312	0.387	0.300	0.304	0.397	0.299
Inj 6	0.214	0.302	0.483	0.191	0.300	0.508

Figure 13: The injection rates applied to numerical simulator. Note there is a frequency exchange between injector 1 and 4, 2 and 5, 3 and 6 on the middle of the period.
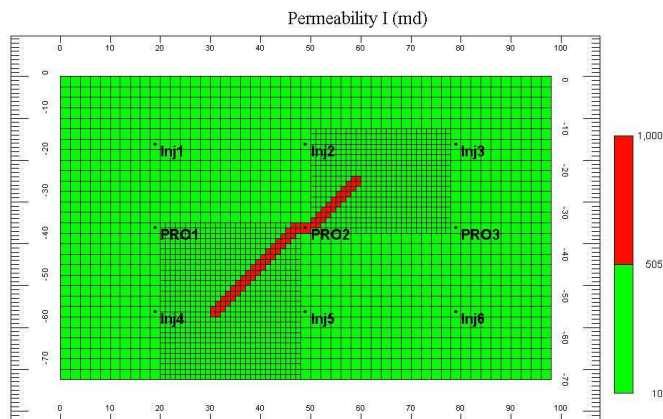

Figure 15: Model on numerical simulator CMG - single layered anisotropic reservoir with 10 md in x direction and 0.01 md in y direction. There is a fracture in the reservoir.
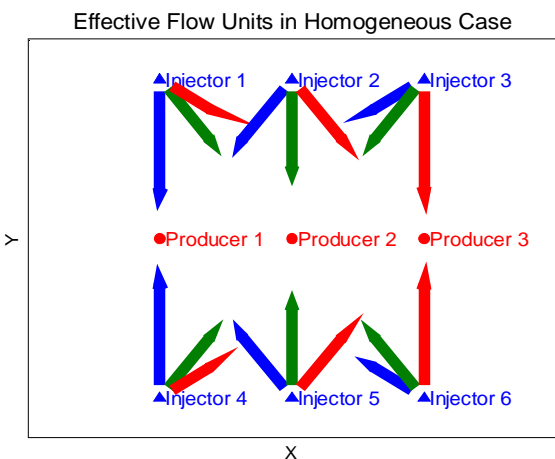

Figure 14: Estimated effective flow units in homogeneous case. The flow units are represented by arrows that start from injector and point to producer in each injector-producer pair. The longer the arrow, the larger value of the effective flow units between the two wells.
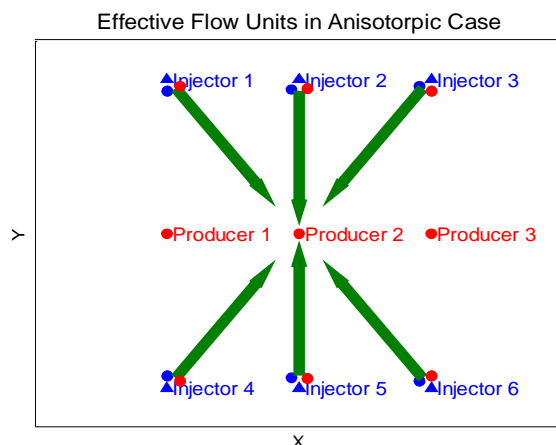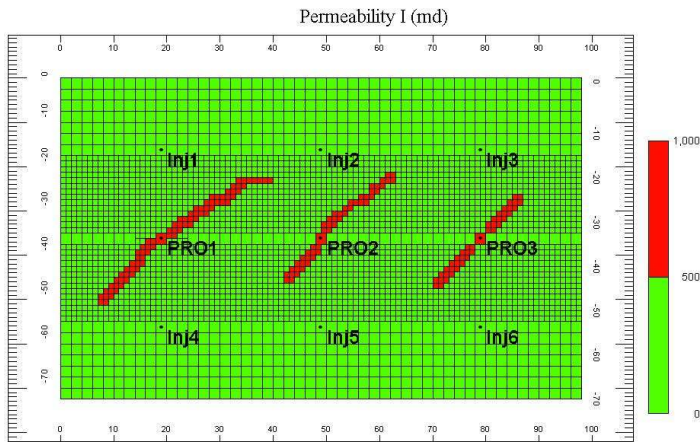

Figure 16: Estimated effective flow units in anisotropic case with single fracture.

Table 2: Estimated effective flow units in anisotropic case plotted in Figure 16.

	First half period			Second half period		
	Pro 1	Pro 2	Pro 3	Pro 1	Pro 2	Pro 3
Inj 1	0.000	1.000	0.000	0.001	0.999	0.000
Inj 2	0.000	1.000	0.000	0.001	0.999	0.000
Inj 3	0.000	1.000	0.000	0.001	0.999	0.000
Inj 4	0.001	0.999	0.000	0.000	1.000	0.000
Inj 5	0.001	0.999	0.000	0.000	1.000	0.000
Inj 6	0.001	0.999	0.000	0.000	1.000	0.000

Table 3: Estimated effective flow units in multiple fractures case plotted in Figure 18.

	First half period			Second half period		
	Pro 1	Pro 2	Pro 3	Pro 1	Pro 2	Pro 3
Inj 1	0.904	0.069	0.027	0.830	0.135	0.035
Inj 2	0.336	0.640	0.024	0.223	0.659	0.118
Inj 3	0.150	0.521	0.329	0.071	0.346	0.583
Inj 4	0.830	0.135	0.035	0.904	0.069	0.027
Inj 5	0.223	0.659	0.118	0.336	0.640	0.024
Inj 6	0.071	0.346	0.583	0.150	0.521	0.329

Figure 17: Model on numerical simulator CMG - single layered reservoir with an isotropic permeability of 0.1 md. There are three fractures wth different length in the reservoir.
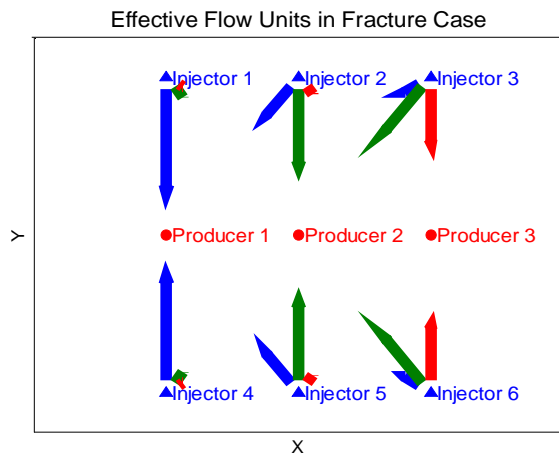
Figure 18: Estimated effective flow units in multiple fractures case.